Dislocation dynamics. II. Applications to the formation of persistent slip bands, planar arrays, and dislocation cells

R. J. Amodeo* and N. M. Ghoniem
Mechanical, Aerospace and Nuclear Engineering Department, University of California, Los Angeles, Los Angeles, California 90024
(Received 10 July 1989)

The dynamic organization of dislocations into spatially heterogeneous substructures is demonstrated by applying the principles of dislocation dynamics that were outlined in the preceding paper. Here it is shown that the formation of persistent slip bands is a consequence of the competition between dipole formation and annihilation of dislocations of opposite Burgers vectors in the absence of temperature-enhanced climb recovery under cyclic stress conditions. Planar arrays, which are also uniaxial structures, are shown to arise from enhanced dislocation multiplication and the formation of stable dipole configurations along a slip plane at lower temperatures where climb is unimportant. Biaxial dislocation systems experience additional degrees of freedom compared with uniaxial systems because of available motion along additional slip systems. It is demonstrated that for a system of orthogonal slip directions at high temperatures in which climb and glide motion are competitive, dislocation cellular structures form as a result of immobile dipole and junction formation and by the internal elastic strain energy minimization caused by long-range self-shielding. It is shown that the internal elastic strain energy is reduced by the self-organization process. However, the short-range nonlinear processes (i.e., dipole and junction formation) are shown not to allow absolute elastic energy minimization.

I. INTRODUCTION

Many different types of dislocation structures have been observed in metals.[1-3] Recently, it was suggested that these structures form as a result of the reduction in free energy of the material systems.[4] Dislocation patterns, called low-energy dislocation structures, are formally defined as any dislocation structure in which neighboring dislocations screen each other's stress field.[1] However, another school of thought suggests that dislocation structures form as a natural consequence of nonlinear interactions among specific dislocation elements within the grain.[5] In general, dislocation structures consist of regions of high dislocation density separated by regions of almost dislocation-free material. The dislocation-rich region is a soft region of facilitated deformation, and the dislocation-poor region is a hard region in which deformation processes do not occur.[6] Even though Argon *et al.*[7] have suggested that the steady-state existence of these structures has not been proved unambiguously, much experimental data[8] verify the constancy of the dislocation density and characteristic dimensions of these structures.

Dislocation structures [i.e., persistent slip bands (PSB's), planar arrays, and cells and subgrains] are found to exist in deforming metals under a variety of experimental conditions.[9] Persistent slip bands are formed under cyclic conditions of stress, and have been mostly observed in copper and copper alloys.[3,10,11] They are essentially uniaxial dislocation structures. They appear as sets of parallel walls, composed of dislocation dipoles which are separated by dislocation-free regions. The length dimension of the wall is orthogonal to the direction of glide of the dislocation.

Dislocation planar arrays are formed under monotonic stress deformation conditions. They are also parallel sets of walls which are composed of sets of dislocation dipoles.[12] While PSB walls are found to be aligned in planes with the normal parallel to the direction of the critical resolved shear stress (CRSS), planar arrays are found to be aligned in planes with the normal perpendicular to the direction of the CRSS.

The dislocation cell structure is a honeycomblike configuration in which there are regions of high dislocation density (the cell walls) and low dislocation density (the region between the walls). Cells can be formed under both monotonic[13,14] and cyclic conditions[2] (the latter occurring after a large degree of cycling has occurred). Direct experimental observations of these structures have been reported for many materials.[15,16] Both theoretical and computational models have been applied to study the formation of many types of dislocation structures.[17]

Current computational models do not accurately treat the dynamics of interaction of a system of dislocations. For example, only long-range forces are considered in the evaluation of dynamic dislocation motion.[18] In recent cellular automata simulations,[19] short-range interactions were included in addition to long-range forces, but a truly dynamical system is not accurately represented in the simulation. Information on the time scale for a simulation of this type is lacking. In Paper I we presented the fundamentals of the newly developed dislocation dynamics (DD) methodology. Here, we show that this methodology resolves some of the problems which exist today

in understanding the phenomena of dislocation pattern formation. We present results on the simulation of these three types of dislocation structures (PSB's, planar arrays, and dislocation cells). These results were obtained by applying the principles of DD to different distributions of dislocations. In the next section we investigate the conditions and characteristics of simulated uniaxial dislocation structures (PSB's and planar arrays). A study of simulated biaxial structures [i.e., two-dimensional (2D) dislocation cells] is then presented in Sec. III. Our conclusions and recommendations for future directions are presented in Sec. IV.

II. SIMULATION OF UNIAXIAL STRUCTURES IN CYCLIC DEFORMATION

The formation of PSB's is represented by the motion of dislocations of only one set of parallel and opposite Burgers vectors. Edge dislocations of opposite Burgers vectors can form dipoles or annihilate. In experimental observations on copper, the climb of dislocations is found to be negligible compared with their glide.[10] This is because experiments of fatigue on copper are usually performed at 25 °C, and at such a low value of temperature that the climb velocity is small compared with the corresponding glide velocity (Fig. 1). Dislocation motion is therefore restricted to glide, and annihilation is only dominant for dislocations whose glide planes are closer than the minimum distance for annihilation. It is also found[10] that the major constituents of PSB walls are edge dislocation dipoles. Screw dislocations annihilate easily by the cross-slip process. We will therefore simulate the formation of banded dipole structures in the study of PSB formation, ignoring the effects of screw dislocations. Another uniaxial structure, the planar array, will also be simulated.

A. Persistent slip bands

The formation of PSB's is a complicated process and occurs in three stages: the formation of loop patches, the formation of the vein structures, and the collapse of the vein structure into PSB's.[11] The simulation which follows is the final stage of this progression.

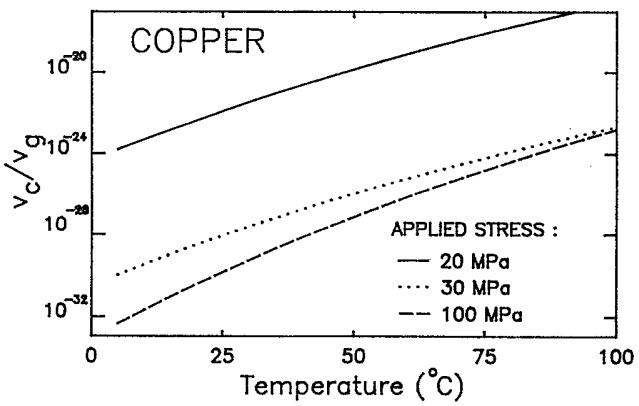

FIG. 1. Ratio of climb to glide velocities for copper.

TABLE I. Slip-band characteristics.

Height of slip-band structure, 10^3 μm
Dipole formation width, 3.5 nm= $13b$
Annihilation width, 1.6 nm = $6.3b$
Dipole density, 4×10^{11}/cm^2
Wall width, 0.1 μm
Wall spacing, 1.4 μm

1. Simulation results

The initial configuration of the vein structure in the simulation is two half veins located at the edges of the simulation space (2.8×1 μm^2), 1.4 μm apart. A periodic boundary condition, in which dislocations leaving either side of the boundary reenter through the opposite side, is applied over the course of the simulation. Table I gives a set of individual parameters for the simulation of PSB's. However, the idealized conditions given in the table did not result in the formation of PSB configurations. Therefore, to simulate the formation of PSB structures, it is necessary to determine the conditions which allow the physics of dislocation interactions to produce banded structures. These conditions are determined by the following parameters: dipole formation width ε_D, dislocation annihilation width ε_a, and friction stress.

We consider a vein structure with a dislocation density of 2.8×10^{10}/cm^2 and 400 dislocations at a temperature of 25 °C. It is found that a dipole formation width of $130b$ and a dipole-to-annihilation ratio of 2.0 are optimal conditions for the formation of slip bands. The fraction of dipoles in the system attains a constant of approximately 50% under these conditions. The fraction of immobile dislocations is shown to decrease as the stress increases, as is expected. The dipole density, on the other hand, peaks at intermediate values of applied stress. At low values of the applied stress, many dislocations immobilize and are therefore incapable of forming dipoles. At intermediate values of stress, the number of immobile dislocations decreases, and many more dislocations are freed up to become dipoles. At very high values of stress, the passing stress for dipole formation is exceeded, resulting in a decrease in the number of dipoles which are capable of reforming. It is found[10] that 15–30 MPa is the optimal applied stress range for the formation of PSB structures.

Experimentally, it is found that the friction stress for pure copper is ≤ 5 MPa.[12] As a function of friction stress at low values of applied stress, the ratio of immobile to total dislocations increases dramatically. This is because at lower values of applied stress, fewer dislocations are capable of surpassing the friction stress. However, if the friction stress is ~ 5 MPa, the fraction of immobile dislocations remains sufficiently low for optimal production of dipoles at any applied stress.

The conditions chosen for the simulation of PSB formation, based on our study, are shown in Table II. The formation of PSB structures without the inclusion of mul-

TABLE II. Data for PSB simulation cases.

Material:	Copper
Dipole width:	$130b$
Annihilation width:	$65b$
Applied stress:	30 MPa
Initial dislocation density:	$2.86\times10^{10}/\text{cm}^2$
Friction stress:	5 MPa
Temperature:	25 °C

tiplication processes is illustrated in Figs. 2(a) and 2(b). The idealized PSB structure is characterized by parallel sets of walls which are perfectly straight. This structure is apparent, however, after many cycles of applied stress. As a material is subjected to forward and reverse stress, the dilocations move with the direction of the applied stress. The result is a temporary wavy-band structure, with centers approximately 1.4 μm apart. In the simulation, dipoles are treated as permanently immobile structures. Therefore after a period of time, the dislocation structure achieves near-static conditions. This is the reason for the appearance of wavy bands, for that is the natural form which initially results from the application of cyclic stress. Figure 2(a) is a demonstration of this effect. After 46 cycles, the bands which form are extremely wavy, indicating the alternating dominance of the applied stress in opposite directions.

Figure 2(b) shows the effect of the slip lamellae, the thin strip of dislocations which is responsible for producing the ladderlike banded structure. In this figure, it is suggested that the mechanism for forming the slip lamellae is the natural breaking through of the wavy-band structure by a set of parallel mobile dislocations. The resultant shearing force causes the isolation of the wavy strips, and eventually they align into the ladderlike structure. It has been suggested by Neumann[20] that once dipoles form, they become movable structures which have an associated mobility. If this is the case, then once the wavy bands are formed, further deformation may result in the alignment of these wavy bands into the ladderlike structure. In the current simulation, however, the wavy bands are composed of immobile dipoles and are therefore incapable of aligning into this configuration.

Figure 3 represents a sequence of a dynamic simulation of PSB formation which shows the transgression from a uniform initial configuration to a distinct wavy-band structure. After 300 time steps, the simulation has proceeded through 8 cycles. Most of the dynamics, however, occur within the first few cycles. The small value of climb velocity is the primary reason for the alignment of the dipoles into banded structures. If two dislocations of the same Burgers vector are stacked on top of each other perfectly vertically, any perturbation would lead to a mutual repulsion of the dislocations because of a net positive force in the glide direction. Dislocations of this type are essentially in a metastable condition. Dislocations of opposite Burgers vectors, however, are in an unconditionally stable configuration if stacked vertically. Since the climb is negligible, dislocations will therefore have a ten-

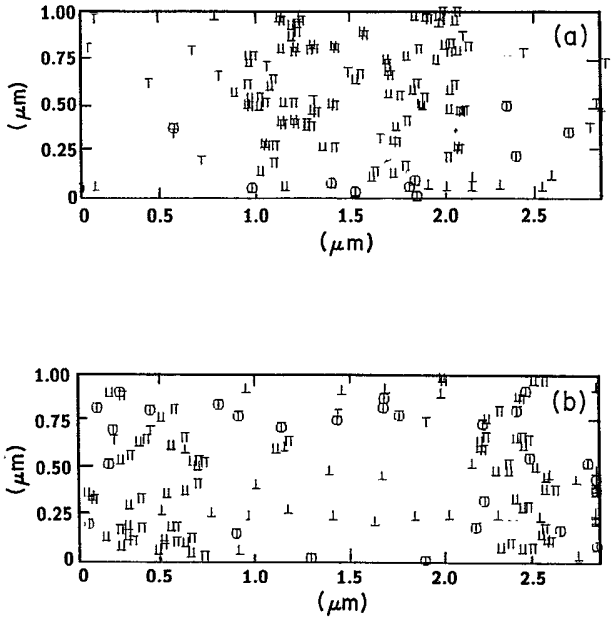

FIG. 2. PSB simulation for copper at 25 °C (see Table II): (a) Elapsed time, 46 s, 1 Hz, 136 dislocations (29 mobile, 11 immobile, 96 dipole); (b) elapsed time, 1 s, 1 Hz, 140 dislocations (37 mobile, 27 immobile, 76 dipole). Symbols are ⊥, mobile edge dislocation; ○, immobile edge dislocation; and ⫫, dislocation dipole.

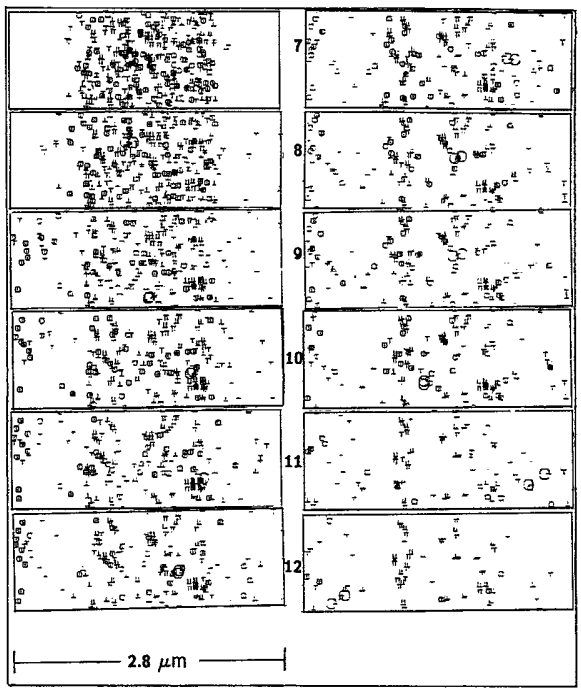

FIG. 3. PSB simulation for copper at 25 °C, 8 cycles ($\sim\frac{2}{3}$ s/frame, 300 iterations). Symbols are ⊥, mobile edge dislocation; ⊕, immobile edge dislocation; and ⫫, dislocation dipole.

dency to form parallel structures, or PSB's.

Although the various components of the local stress tensor can be computed at any dislocation, we will only focus on the shear component acting on the glide plane, τ. We introduce the following definitions:

$$\tau_i^{\text{int}} = \sum_{\substack{j=1 \\ j\neq i}}^{N} \tau_{ij} , \tag{1}$$

$$\tau_i^{\text{eff}} = \tau_i^{\text{int}} - \tau_0 , \tag{2}$$

$$\langle \tau^{\text{int}} \rangle = \frac{1}{N} \sum_{i=1}^{N} \tau_i^{\text{int}} , \tag{3}$$

$$\langle \tau^{\text{eff}} \rangle = \frac{1}{N} \sum_{i=1}^{N} \tau_i^{\text{eff}} , \tag{4}$$

where the local internal stress at dislocation i is denoted by τ_i^{int}, mutual elastic stress between dislocations i and j is τ_{ij}, the friction stress is τ_0, the effective stress at dislocation i is τ_i^{eff}, and averages are represented by the symbol $\langle\ \rangle$.

Figure 4 is a plot of the evolution of the average effective and internal stresses during the simulation. It shows that there is a tendency for the average internal stress to be reduced because of the organization of dislocations into a more regular structure. The effective and internal stresses follow approximately the same path of evolution up to about 120 time steps. The value of the effective stress then saturates while the internal stress continues to decrease. The effective stress exceeds the internal stress by a value on the order of the difference between the applied stress and the friction stress. The net internal stress for mobile dislocations within the effective stress averages out to zero. This means that for every mobile dislocation, there exists another in the system with opposite internal stress. The reason for the difference between the effective and internal stresses is that once a stable PSB structure has formed, the mobile dislocations present in the system are screened from each other by dislocations which constitute organized structures. This appears to occur very early during stress cycling.

Figure 5 is a plot of the evolution of the total number

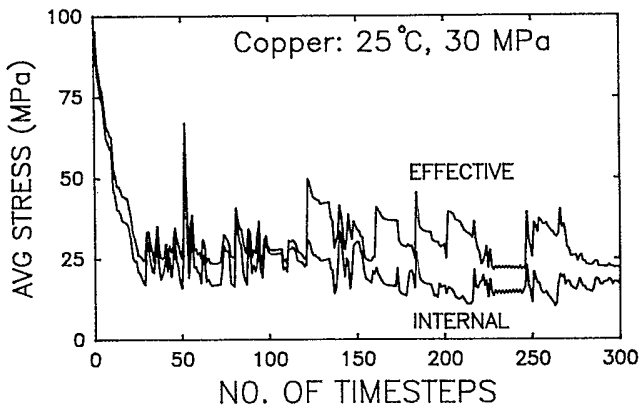

FIG. 4. Evolution of internal and effective stresses for PSB simulation (total time is 8 s).

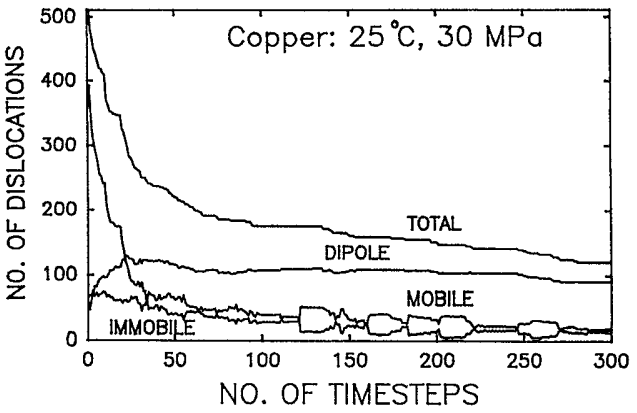

FIG. 5. Evolution of dislocation species for PSB simulation (total time is 8 s).

of dislocations as a function of time (or number of computational time steps). It can be seen that the relaxation phase occurs fairly early in the simulation, and that the dipoles which form the PSB wall do so rather rapidly. The cycling frequency for this simulation experiment was taken to be 2 Hz, and the total number of cycles corresponding to 300 iterations was 46. Once the dipole structures form, further condensation into distinct PSB structures occurs because of the annihilation of mobile dislocations which are still present in the vein structure. This can be seen very clearly in Fig. 3.

2. *Effects of dislocation multiplication*

Dislocation multiplication is possible if the Orowan criterion (outlined in Paper I) is satisfied. If the stress on a dislocation along a glide plane exceeds the Orowan stress, then multiplication occurs. To study the effects of dislocation multiplication, we divide the vertical axis into 20 strips of equal width and apply a cyclic stress to the material. Each strip represents a number of glide planes. If the Orowan criterion is satisfied along a strip, then we limit the time step to allow for the production of, at most, two dislocations. The resultant configuration is seen in Fig. 6, which depicts a slip-band pattern forming coincident with a strip, or slip lamellae, produced by dislocation multiplication. This strip is composed of roughly equal numbers of dipole and mobile dislocations. In Fig. 7, it is seen that the dislocation dipoles form rapidly in the evolution of the structure. There is a balance between dislocation annihilation and dipole formation in these early stages. After the population of dipoles has reached its steady state, new dislocations are produced which contribute to the annihilation process. It has been suggested that these dislocations which annihilate with the primary dislocations in the vein are actually secondary dislocations which are activated by the critical conditions of stress and temperature.[10] The simulations suggest that whatever the mechanism for generation of dislocations, annihilation and dipole formation are two key processes which are responsible for the formation of PSB's and slip lamellae.

Persistent slip-band structures are caused by disloca-

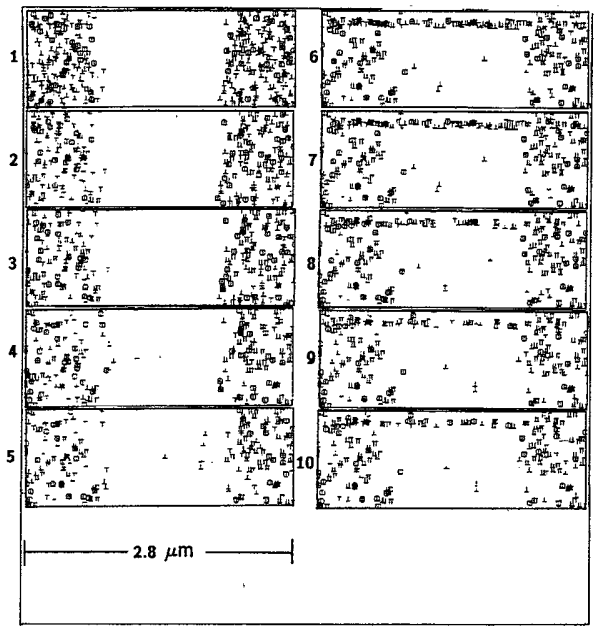

FIG. 6. Dynamic simulation of PSB formation including strip multiplication for copper at 25 °C, 1 cycle ($\frac{1}{10}$ s/frame, 300 iterations). Symbols are ⊕, mobile edge dislocation; ⊥, immobile edge dislocation; and ⫫, dislocation dipole.

tion processes which do not depend on the crystal structure.[21] These PSB's are observed in many materials such as low carbon steels, precipitation-hardened alloys, and pure fcc metals.[21] Our computer simulations are consistent with the experimental observations of PSB formation by Essmann and Mughrabi[22] and by Mughrabi.[23]

B. Planar arrays

Planar arrays have been referred to in a general sense as any alignment of dislocations along one specific direction, whether it is parallel or orthogonal to the Burgers vector of constituent dislocations. In this section, however, we will consider planar arrays as those structures containing parallel dislocations with Burgers vectors parallel to the direction of the critical resolved shear stress. This situation corresponds to the propagation of slip under shear loading. It has been suggested that planar arrays arise from enhanced dislocation multiplication due to alloying elements in the matrix.[12] The initially high density of dislocations is followed by an almost spontaneous increase in dislocation population along one specific plane. Several nucleation points subsequently develop, resulting in a set of parallel dislocations comprising groups of dislocation dipoles. It is common for planar arrays to group together in band configurations, although the reasons are not entirely understood.[12] Once a single band forms, the nucleation process for an adjacent band is possible and appears to occur roughly 0.5 μm away from the original band. Other bands can also form far away from the first band. It is possible that the formation of these bands is dependent upon random nucleation sites which form within the material.

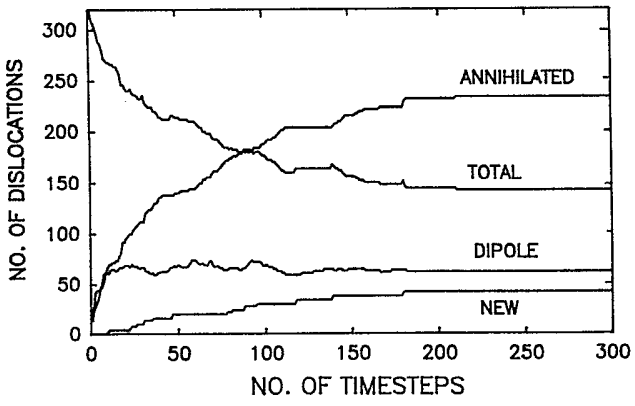

FIG. 7. Evolution of dislocation species during random multiplication (total time is 3 s).

In simulating the formation of planar arrays, we consider a rectangular space 4×2 μm^2 with an initial random distribution of 400 dislocations within this space. We then subdivide the vertical axis into a number of strips within which we allow multiplication to occur. It should be recalled that this type of production is an autocatalytic multiplication process subject to the Orowan stress criterion within each strip. Once a sufficient number of dislocations has been produced, the Orowan stress criterion no longer becomes satisfied within the region and dislocation production ceases. Dislocations leaving the system are allowed to reenter on the opposite side, thus constituting a periodic boundary condition. The parameters for this simulation are the same as those used in the simulation of the PSB's (Table II), except with an initial dislocation density of $5.0\times10^9/cm^2$. The total simulation time is less than one second.

Figure 8 is a progression of a planar array simulation for the above conditions with 20 subdivisions of the vertical axis for dislocation multiplication. These figures are separated by approximately ten iterative steps of simulation time. The first frame is the initial configuration which is composed of mostly immobile dislocations. In the second frame much annihilation occurs within the matrix, especially at the bottom of the figure. The Orowan criterion is then satisfied for this top region, and dislocation multiplication can occur. In the third frame, we observe the multiplication in this region, and a high concentration of dipoles within the strip. In the fourth frame at the top of the figure, a second nucleation point has occurred roughly 4.0 μm away from the original strip. Meanwhile multplication has rapidly ceased within the bottom strip and dynamic recovery occurs within this strip. In the fifth frame, both bands experience recovery. In the sixth frame, a new set of dislocations has been produced a little more than 0.5 μm away. In the seventh frame, all three bands form relatively stable dipolar array structures. Finally, in the eighth frame, about 0.5 μm away from the third band, another band nucleates from the existing structure. This last frame is a very interesting display of planar array formation because it contains many of the characteristics of the experimental observa-

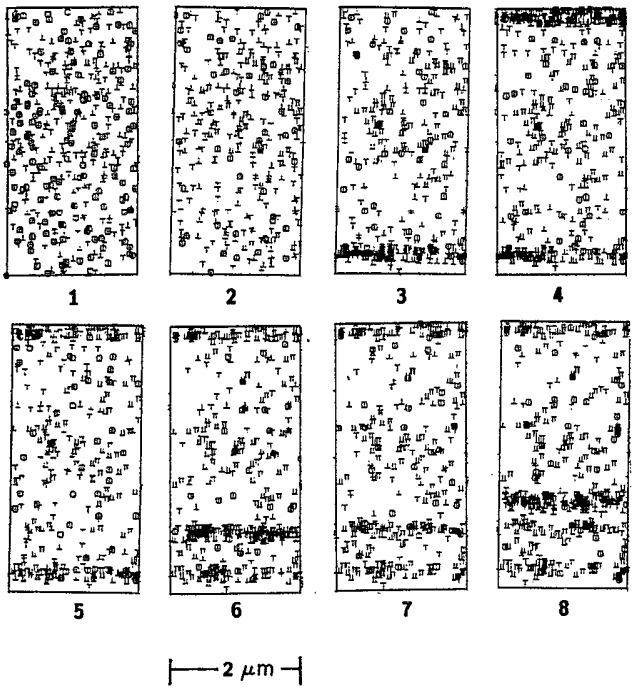

FIG. 8. Planar array simulation for copper at 25 °C, 1 cycle ($\frac{1}{8}$ s/frame, 300 iterations). Symbols are ⊥, mobile edge dislocation; ⏀, immobile edge dislocation; and ⫫ dislocation dipole.

tions of Neuhäuser, Arkan, and Potthoff,[12] and the more recent results of Olfe and Neuhäuser.[24] The formation of planar arrays is achieved from the high rate of heterogeneous multplication and the formation of stable dipole structures along a slip plane.

III. SIMULATION OF BIAXIAL STRUCTURES IN MONOTONIC DEFORMATION

The experimental conditions which lead to cell formation differ from those which allow the formation of PSB's. For cells, application of higher temperatures allows greater dislocation mobility due to enhanced glide and the operation of dislocation climb (Fig. 9). In a biaxial structure, there are two independent sets of glide planes. In this section we consider the formation of 2D structures (dislocation cells) in a biaxial (two axes of glide) simulation of dynamic processes.

Dislocation cell walls can comprise two or three sets of Burgers vectors.[25] The motion of dislocations of different Burgers vectors occurs in three separate directions. Since we are cutting a slice of the material and observing dislocations in two dimensions, it would appear difficult to simulate the true motion of dislocations. However, considering that the system of dislocation cells is isotropic in three Cartesian directions, we can represent the projection of the dislocation motion of two of the Burgers vectors in the plane of observation. Since the dislocation is a long line of discontinuity, and not actually a "link," a dislocation will not move out of the plane of observation. Hence the motion of the projection of the dislocation line will always be properly represented in the 2D plane of ob-

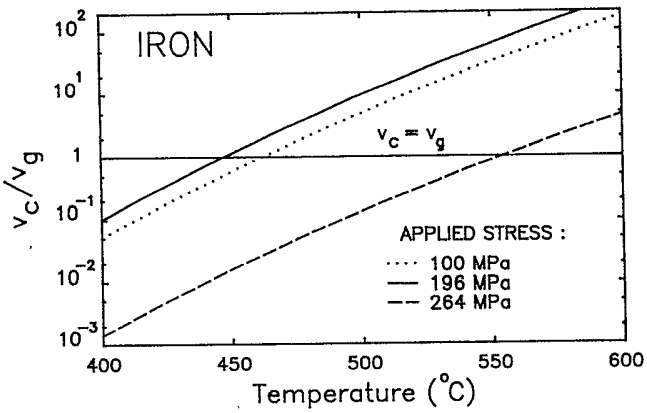

FIG. 9. Ratio of climb to glide velocities.

servation. In the current biaxial simulation, we consider a system of two orthogonal glide directions for dislocation motion. This reduces the complexity of the simulation, and represents a more accurate interpretation of the projection of dislocation lines onto the observation plane.

The following are results of a simulation of the progression from a uniform entanglement of dislocations to the formation of organized cellular structures. The material is subjected to a cumulative strain within the primary range of the dislocation creep, and it is assumed that a critical number of dislocations have already been produced. The following stage is the collapse of the dislocation structure into the cellular configuration. This happens within a short time span ($\sim$1 s to 1 h) depending upon initial conditions. Once the cells form, they exist as stable structures for a short period until coarsening occurs and they coalesce into subgrain structures. In the current study we consider only the initial stages of cell formation. The material considered in this study is alpha-iron. All of the cases studied in the following computer experiments consist of 1 square micron of the microstructure containing 400 dislocations (dislocation density: $4\times10^{10}/\text{cm}^2$). The dislocations are oriented with their Burgers vectors aligned with the corresponding diagonals of the square. Therefore there are a total of four different types of dislocations, or two sets of dislocation systems with orthogonal Burgers vectors. A monotonic stress is applied in the positive x direction. The temperature is varied between 400 and 600 °C and the applied stress is varied between 100 and 400 MPa.

It is found that performing a simulation beyond the limits of these parameters does not produce organized structures. The computer simulation for the case of high temperature (600 °C) and high stress (440 MPa) results in a cluster of dislocation multipoles which forms rapidly, while mobile dislocations which do not form dipoles experience annihilation by climb processes. On the other hand, a simulation at low temperatures (400 °C) and low stress (100 MPa) leads to the formation of a large number of immobile dislocations. This happens because the applied stress is much lower than the friction stress. Finally, at low temperature (400 °C) and high stress (250 MPa), but with a much lower value of dislocation density

TABLE III. Data for dislocation cell simulation cases.

Material:	Iron
Dipole width:	$130b$
Annihilation width:	$65b$
Junction width:	$40b$
Applied stress:	100 MPa
Initial dislocation density:	$4.0\times10^{10}/\text{cm}^2$
Friction stress:	14 MPa
Temperature:	600 °C
Initial no. of dislocations:	400
Dimensions:	1 μm^2

($\sim1.4\times10^{10}$ cm^2), the computer simulation produces a collection of mostly mobile dislocations in a loosely knit cellular configuration. Table III is a list of the parameters used in the study of dislocation cell formation.

Figure 10 is a simulation of the formation of dislocation cellular structures under creep conditions [high temperature (600 °C) and low stress (100 MPa)]. In this simulation, it is seen that a cellular structure rapidly forms. The cell sizes are on the order of 0.5 μm, which is somewhat lower than that expected from average conditions described by Holt's relationship between dislocation density and cell radius.[26] The experimental value of the average cell diameter corresponding to this equation is on the order of 1 μm for the given initial conditions. The resulting configuration contains a total of 210 dislocations, of which 206 are immobilized dislocations; 93 are immobile, 20 are dislocation dipoles, and 84 are junction dislocations. The boundaries of the cells are primarily composed of dipole or junction dislocations. It appears that

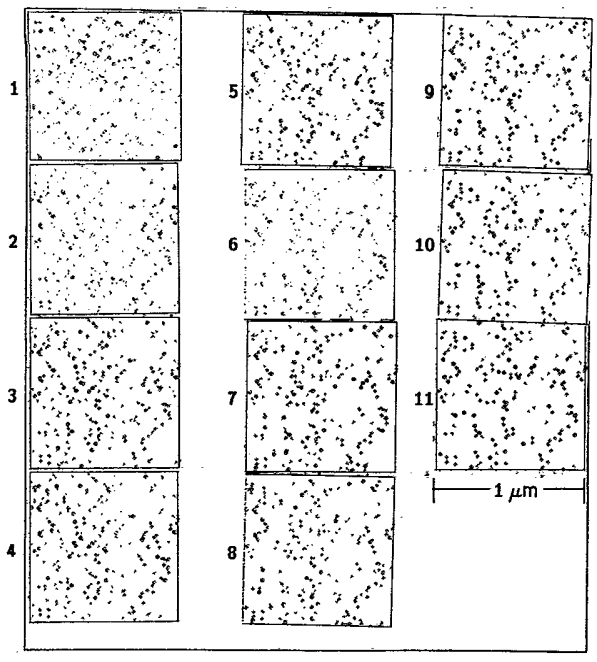

FIG. 10. Simulation of cell formation: Iron at 600 °C, 100 MPa, $4\times10^{10}/\text{cm}^2$ (~1 s/frame). Symbols are ⊥, mobile edge dislocation; ⊕, immobile edge dislocation; and ⫫, dislocation dipole.

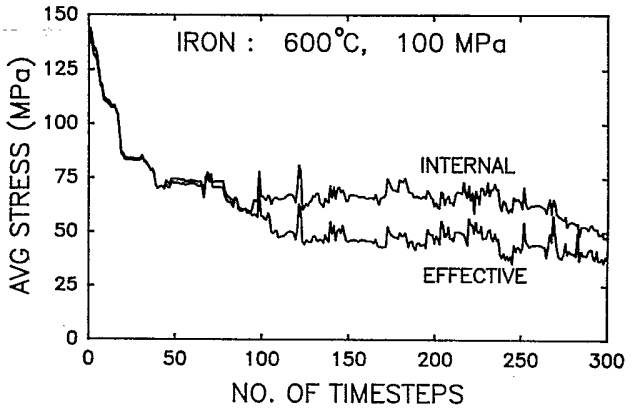

FIG. 11. Evolution of internal and effective stresses for the simulation of cell formation (total time is 10 s).

the formation of the cellular structure is therefore critically dependent upon the total number of immobilized dislocations, in particular stable immobile dislocations.

Figure 11 shows the average internal and effective stresses of mobile dislocations as functions of time for a typical case. Initially, dislocations are randomly distributed throughout the medium. There is a general tendency for the reduction of the elastic stresses due to the rearrangement of dislocations into screened configurations. The effective stress follows the internal stress due to the averaging out of the applied and friction stresses for a stochastically random configuration. It should be recalled that the friction stress opposes the glide velocity in whichever direction the dislocation is gliding. This is why the friction stress averages to zero in the initial random configuration. The applied stress is actually dependent upon the angle of orientation of the dislocation with respect to the x axis. For a single dislocation, the applied stress is given by $\sigma=\sigma_a\cos\alpha$. Thus integrating this over all angles results in an average applied stress of zero.

After about 90 time steps of the simulation, it is interesting to observe that the internal stress bifurcates from the effective stress, and the two are separated by a nearly constant value until the end of the simulation. The steady-state value of internal stress approximately assumes the value of the effective critical resolved shear stress. The value of the effective stress approaches the difference between the internal stress and the friction stress. At this point, a cellular configuration has formed, and mobile dislocations are effectively screened from each other by the effect of the cell boundary.

Figure 12 is a history of the evolution of dislocation types within the cell as a function of time. Initially, we begin with 400 dislocations which experience a relaxation phase due to inherent inhomogeneities. These inhomogeneities are resolved by dynamic recovery in the initial phase, and we are left with approximately 300 dislocations to begin with. The total number of dislocations decreases as a function of time, due specifically to annihilation by glide and climb processes. The total number of immobilized dislocations increases steadily as time proceeds, and eventually dominates the composition of dislocations within the square cell. After about 90 time

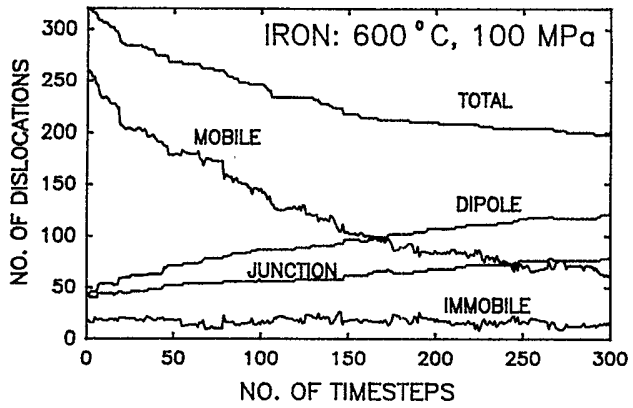

FIG. 12. Evolution of dislocation species for the simulation of cell formation (total time is 10 s).

steps, the fraction of dislocations which are immobilized (i.e., junctions, immobile dislocations, or dipoles) is 50%. Once the density of immobilized dislocations begins to dominate the material, then cellular configurations can form.

Stable cell structures have been observed at lower homologous temperatures during deformation, while subgrains ultimately develop at higher temperatures.[27] Direct experimental observations of dislocation cells have been reported for many materials.[13,15,16,28–31] Our computer simulations of dislocation cells show the general features of experimentally observed structures. It is worth noting here that the computational techniques can be made more efficient, and future developments should allow the simulation of more involved dislocation interaction physics. Examples of efficient computational techniques are given in Ref. 32.

IV. CONCLUSIONS

Computer-simulation results indicate that slip-band structures are likely to form if the stress and temperature conditions are favorable for competition between dipole formation and dislocation annihilation. It is found that the formation of short-range dipolar structures early in the simulation is critical for the formation of PSB structures. A low concentration of immobile dislocations is necessary to allow a significant production of dipoles within the PSB structure, and at the same time provide stability points for the collection of dipoles. At a value of the friction stress of approximately 5 MPa, the fraction of immobile dislocations is sufficiently low to ensure the optimal production of dipoles for any applied stress. Other mechanisms, such as the enhancement of annihilation by the presence of secondary dislocations, may also be responsible for triggering the collapse of vein structures into slip bands.

In the simulation, the structure of PSB's after the collapse of the vein is generally a wavy-band structure with centers approximately 1.4 μm apart. This is because a material is subjected to forward and reverse stresses, and the dislocations move with the direction of the applied stress. Once dipoles form, they are treated as immobile structures which are incapable of being remobilized. If, as Neumann suggests, dipoles have a characteristic mobility and can also be swept, then once the wavy bands are formed, further deformation may result in the alignment of these wavy bands into the ladderlike structure.

It is found that two different mechanisms may be responsible for the formation of slip lamellae. One suggested mechanism is the natural breaking through of the wavy-band structure of a set of parallel mobile dislocations. The other is the multiplication of dislocations along a strip in which the Orowan criterion for dislocation multiplication is satisfied. In both cases, the resultant shearing force eventually causes the isolation of the wavy strips, and eventually they align into the ladderlike structure. Another effect of multiplication is to provide a source of dislocations for the annihilation of dislocations within the vein structure.

The small value of climb velocity is the primary reason for the alignment of dipoles into banded structures. Since climb is negligible at low temperatures, dislocations in a stacked configuration are in a metastable condition. Because dislocations have formed dipolar configurations within the PSB, they have essentially stabilized after the alignment of the dislocations has occurred. In general, however, the balance between annihilation and dipole formation is the key to the actual formation of these structures. The formation of planar arrays, on the other hand, is dependent upon heterogeneous multiplication processes and the stability of dipole structures along a slip plane.

The formation of cellular structures is found to be critically dependent upon the total number of immobilized dislocations, in particular stable immobile dislocations. Initially, dislocations are uniformally distributed throughout the medium. The initial driving force for cell formation is the tendency of the system to reduce the total elastic strain energy through the reduction of the internal stresses by a rearrangement of dislocations into a more shielded configuration. The effective stress follows the internal stress due to zero averaging of both the applied and friction stresses for a stochastically random configuration. Nonlinear reactions, such as dipole and junction formation, do not permit this complete relaxation of the elastic strain energy. The average internal stress relaxes to a value on the order of the applied stress, which is consistent with a cell diameter that is inversely proportional to the applied stress, as observed experimentally. It is to be noted that the climb mobility of dislocations must still be sufficiently high for dislocation cells to form.

It is found that the tendency to form one type of organized structure or another is dependent upon the material which is subjected to the conditions of applied stress and temperature. This is because the relative speed of dislocations in the climb and glide directions is an important contributing factor in the formation of organized spatial dislocation structures. For iron, it is seen (Fig. 9) that the climb velocity is dominant at high temperature and low-to-intermediate stress, whereas the glide velocity is dominant in the low-temperature–high-stress range. Under conditions of dislocation creep, where cellular dislocation

patterns are likely to form, climb motion plays a central role. For copper, however, it appears (Fig. 1) that glide is the predominant mechanism. For values of applied stress above 30 MPa, the ratio of climb to glide reaches a saturation value. For applied stresses below 30 MPa, the climb begins to become more significant. At even lower values of applied stress, the climb velocity actually becomes greater than the glide velocity.

For both uniaxial structures (PSB's) and biaxial structures (dislocation cells) it is found that the value of the average internal and effective stresses bifurcate after organization occurs. In the early stages where the dislocation configuration is still random, these stresses are identical because the average values of the applied and friction stresses are zero. After a sufficient number of dislocations agglomerate into organized patterns, the dislocations existing within the cells are screened from dislocations outside the cell boundaries. The bifurcation of the internal and effective stresses occurs at this point, because a sufficient number of dislocations is immobilized. Although the organized configuration is of lower energy compared to the initial random distribution, it nevertheless is constrained by the nonlinearities inherent in dislocation reactions. The term low-energy dislocation configuration should therefore be used with caution, for a minimization of the elastic strain energy is not a sufficient criterion for the formation of dislocation structures.

ACKNOWLEDGMENTS

This work was supported by the U.S. Department of Energy, Office of Fusion Energy, Grant No. DE-FG03-84ER52110, with UCLA.

*Current address: Xerad Inc., 1526 14th Street, Suite 102, Santa Monica, CA 90404.

[1]D. Kuhlmann-Wilsdorf, Mater. Sci. Eng. **86**, 53 (1987).
[2]L. Yumen and Z. Huijiu, Mater. Sci. Eng. **81**, 451 (1986).
[3]K. Lepisto, V. T. Kuokkala, and P. O. Kettunen, Mater. Sci. Eng. **81**, 457 (1986).
[4]Mater. Sci. Eng. **81**, 1 (1986).
[5]D. Walgraef and E. Aifantis, Int. J. Eng. Sci. **23**, 1351 (1985).
[6]A. Orlova and J. Cadek, Mater. Sci. Eng. **77**, 1 (1986).
[7]A. S. Argon, F. Prinz, and W. C. Moffatt, in *Dislocation Creep in Subgrain-Forming Pure Metals and Alloys,* edited by B. Wilshire and D. R. J. Owen (Pineridge, Swansea, 1981), p. 1.
[8]S. Takeuchi and A. S. Argon, J. Mater. Sci. **11**, 1542 (1976).
[9]M. Pahutova, J. Cadek, and V. Cerny, Mater. Sci. Eng. **62**, 33 (1984).
[10]H. Mughrabi, Mater. Sci. Eng. **33**, 207 (1978).
[11]C. Laird, P. Charsley, and H. Mughrabi, Mater. Sci. Eng. **81**, 433 (1986).
[12]H. Neuhäuser, O. B Arkan, and H. H. Pothoff, Mater. Sci. Eng. **81**, 201 (1986).
[13]B. Reppich, J. Mater. Sci. **6**, 267 (1971).
[14]A. Orlova, M. Pahutova, and J. Cadek, Philos. Mag. **25**, 865 (1972).
[15]F. Garofalo, L. Zwell, A. S. Keh, and S. Weissmann, Acta Metall. **9**, 721 (1961).
[16]G. Streb and B. Reppich, Phys. Status Solidi A **16**, 493 (1973).
[17]R. Amodeo and N. M. Choneim, Res Mechanica **23**, 137 (1988).
[18]W. W. Gerberich, E. Kurman, and W. Yu, in *The Mechanics of Dislocations,* edited by E. Aifantis and J. Hirth (American Society for Metals, Metals Park, OH, 1983), pp. 169–179.
[19]J. Lepinoux and L. P. Kubin, Scripta Metall. **21**, 833 (1987).
[20]P. Neumann, Z. Metallkd. **59**, 927 (1968).
[21]L. M. Brown, Met. Sci. J. **11**, 315 (1977).
[22]U. Essmann and H. Mughrabi, Philos. Mag. **40**, 731 (1979).
[23]H. Mughravi, Acta Metall. **31**, 1367 (1983).
[24]J. Olfe and H. Neuhäuser, Phys. Status Solidi A **109**, 149 (1988).
[25]D. Caillard and J. L. Martin, Acta Metall. **30**, 791 (1982).
[26]D. Holt, J. Appl. Phys. **41**, 3197 (1970).
[27]H. Mughrabi, in *Constitutitive Equations in Plasticity,* edited by A. S. Argon (MIT Press, Cambridge, MA, 1975), p. 327.
[28]J. L. Lytton, C. R. Barrett, and O. D. Sherby, Trans. Metall. Soc. AIME **23**, 1399 (1965).
[29]V. P. Gupta and P. R. Strutt, Can. J. Phys. **45**, 1213 (1967).
[30]B. L. Jones and C. M. Sellars, Met. Sci. J. **4**, 96 (1970).
[31]A. C. Clauer, B. A. Wilcox, and J. P. Hirth, Acta Metall. **18**, 381 (1970).
[32]N. M. Ghoneim and R. J. Amodeo, Solid State Phenom. **304**, 377 (1988).